Local phase space control and interplay of classical and quantum effects in dissociation of a driven Morse oscillator

Astha Sethi and Srihari Keshavamurthy
Department of Chemistry, Indian Institute of Technology, Kanpur 208 016, India
(Received 17 September 2008; published 26 March 2009)

This work explores the possibility of controlling the dissociation of a monochromatically driven one-dimensional Morse oscillator by recreating barriers, in the form of invariant tori with irrational winding ratios, at specific locations in the phase space. The control algorithm proposed by Huang *et al.* [Phys. Rev. A **74**, 053408 (2006)] is used to obtain an analytic expression for the control field. We show that the control term, approximated as an additional weaker field, is efficient in recreating the desired tori and suppresses the classical as well as the quantum dissociation. However, in the case when the field frequency is tuned close to a two-photon resonance the local barriers are not effective in suppressing the dissociation. We establish that in the on-resonant case quantum dissociation primarily occurs via resonance-assisted tunneling and controlling the quantum dynamics requires a local perturbation of the specific nonlinear resonance in the underlying phase space.

DOI: 10.1103/PhysRevA.79.033416 PACS number(s): 33.80.Wz, 33.80.Gj, 05.45.Gg

I. INTRODUCTION

For over three decades the one-dimensional driven Morse oscillator [1] has served as a fundamental model to understand and elucidate the dissociation mechanism of diatomic molecules. The continued interest in this seemingly simple system is due to two main reasons. First, the hope is that insights into the mechanism can be utilized to understand infrared multiphoton dissociation of polyatomic molecules [2–4] and related phenomena including vibrational predissociation [5] and mode-specific dynamics [6,7]. Second, at present the focus of researchers is increasingly shifting from gaining mechanistic insights to controlling [8–11] the various processes and in this regard a firm understanding of the underlying mechanisms is essential. Therefore, it is not entirely surprising that the driven Morse system has been studied in great detail from the quantum, classical, and semiclassical [12] perspectives and with an equally diverse choice for the field-monochromatic [13–22], bichromatic (with relative phase) [23–30], chirped [31–34], shaped pulses [21,26,35], and stochastic noise [36]. More recently, the dynamics of a Morse oscillator under the influence of external fields has become relevant in the context of models for quantum computing based on molecular vibrations [37].

A majority of the studies have addressed the problem from a classical-quantum correspondence viewpoint; a knowledge of the regimes where classical or quantum mechanisms are appropriate and regimes where they coexist and compete is crucial for control [38]. Several important insights have originated from such efforts which have established that molecular dissociation, in analogy to multiphoton ionization of atoms [39–41], occurs due to the system gaining energy by diffusing through the chaotic regions of the phase space. For example, an important experimental study by Dietrich and Corkum [42] has shown, among other things, the validity of the chaotic dissociation mechanism. Thus, the formation of the chaotic regions due to the overlap [43] of nonlinear resonances (field-matter), hierarchical structures [44,45] near the regular-chaotic borders acting as partial barriers, and their effects on quantum transport [46] have been studied in a series of elegant papers [15,48,47]. A general consensus, at least for the one-dimensional driven Morse system, is that classical-quantum correspondence holds up rather well except in the regimes of quantum multiphoton resonances [13,16–18,33].

A recurring theme in many of the works on driven Morse system has to do with enhancing the dissociation. The search for ways to efficiently dissociate the molecule has led to a variety of suggestions like bichromatic fields with the relative phase as a control knob [23,24,28–30], frequency-chirped fields [31], and resonant stimulation [49]. However, there are instances wherein one is interested in suppressing the dissociation rather than enhancing it. This is important, for example, in the context of vibrational quantum computing [37] where loss of population into states other than the states of interest compromises the efficiency of the quantum gates. Another example comes from coupled Morse oscillator systems where it might be necessary to keep one of the modes "quiet" in order to carry out mode-specific dynamics [4]. A powerful approach to implement such constraints on the system comes from optimal control theory [50] (OCT) and indeed driven Morse oscillator systems provide an ideal testbed for OCT-based schemes [51]. Yet, in our opinion, it is worthwhile addressing the issue from a classical-quantum correspondence perspective as well. Not only is it natural, given the extensive insights that classical mechanics can provide, but it might also provide a useful way of decoding information buried in an otherwise complicated optimal field coming out of an OCT calculation. Similar considerations are at the heart of several works [52] aimed at understanding the dynamical origins of the control fields.

Since a detailed understanding of the role of various phase space structures in the driven Morse system already exists, is it possible to use the phase space information to control the dissociation using additional, hopefully simple, fields? Recently, a similar question was addressed by Huang *et al.* [53] in the context of suppressing the multiphoton ionization of atomic systems. Using methods [54] developed in

a different context, it was found that the ionization process could be suppressed by rebuilding some of the broken invariant tori at carefully chosen locations in the phase space. Inspired by their approach, and noting the mechanistic similarities between molecular dissociation and atomic ionization [55], in this work we attempt to control the dissociation of a monochromatically driven Morse oscillator using the local control algorithm. In their study, Huang *et al.* [53] focused only on the classical aspects of suppressing the ionization. It is, however, important to ask if the classical barriers are effective quantum mechanically as well since it is not immediately clear that local barriers in the phase space translate to local suppression of quantum dynamics. We address this issue using the driven Morse system and show that phase space barriers, especially cantori, do inhibit both classical and quantum dissociation. As one would expect, such good classical-quantum correspondence fails in the case of two-photon resonance. However, we show that the complication comes from a subtle interplay between classical and quantum mechanisms with resonance-assisted tunneling [56–58] playing a key role.

We begin by describing some of the salient features of the driven Morse oscillator in Sec. II. After a brief description of the methodology, Sec. III contrasts the dissociation dynamics in the off-resonant and on-resonant situations and a specific initial Morse state is identified to be subjected to the local control strategy. In Sec. IV, we give a brief summary of the local control method resulting in an analytic form of the control field. A simplified control field, appropriate for classical-quantum correspondence studies, is obtained. The efficiency of the simplified control term in recreating various cantori barriers in phase space and hence controlling the classical and quantum dissociation dynamics is shown and discussed in Sec. V. In the same section we illustrate the importance of resonance-assisted tunneling in the on-resonance regime. Finally we conclude in Sec. VI with some comments on the method, possible generalizations, and future applications.

II. MODEL HAMILTONIAN

The driven Morse oscillator, modeling the dissociation of a diatomic molecule by linearly polarized laser fields, is described [15] by the Hamiltonian

$$H(x,p;t) = H_0(x,p) - \lambda_1 \mu(x)\cos(\omega_F t), \tag{1}$$

with the unperturbed Hamiltonian

$$H_0(x,p) = \frac{1}{2M}p^2 + D_0[1 - e^{-\alpha(x-x_e)}]^2, \tag{2}$$

corresponding to a one-dimensional Morse oscillator. It is well known that H_0 provides a good model for describing the anharmonic vibrations of diatomic molecules with D_0, α, x_e, and M being the dissociation energy, range of the potential, equilibrium position, and the reduced mass of the molecule, respectively. The bound eigenstates and eigenvalues corresponding to the Hamiltonian $H_0(x,p)$ can be expressed, with $z \equiv 2ae^{-\alpha(x-x_e)}$, as [59]

$$\chi_\nu(z) = \sqrt{\frac{\alpha(2a-1-2\nu)\nu!}{\Gamma(2a-\nu)}}e^{-z/2}z^{b_\nu}L_\nu^{2b_\nu}(z), \tag{3a}$$

$$E_\nu = \frac{2D_0}{a}\left(\nu+\frac{1}{2}\right) - \frac{D_0}{a^2}\left(\nu+\frac{1}{2}\right)^2, \tag{3b}$$

where $L_\nu^{2b_\nu}(z)$ is the generalized Laguerre polynomial, $a = \sqrt{2MD_0}/\alpha\hbar$ and, $b_\nu = \sqrt{2(D_0 - E_\nu)M}/\alpha\hbar$. Since this work is concerned with studying dissociation caused by fields of moderate intensity, a linear approximation for the dipole function

$$\mu(x) \approx \mu(x_e) + \left(\frac{\partial\mu}{\partial x}\right)_{x_e}(x-x_e) \equiv \mu(x_e) + d_1(x-x_e) \tag{4}$$

is valid as long as the qualitative nature of the classical and quantum dynamics are unaltered as compared to working with the full dipole function $\mu(x)$. Moreover, as seen later, the linear form allows for a relatively easier implementation of the local control algorithm [54] in terms of deriving analytic expressions for the control field.

Given that this work focuses on suppressing dissociation by creating robust Kolmogorov-Arnol'd-Moser (KAM) tori in the phase space, the action-angle variables (J,θ) of the unperturbed Morse oscillator

$$J = \sqrt{\frac{2MD_0}{\alpha^2}}(1 - \sqrt{1-E}), \tag{5a}$$

$$\theta = -\,\mathrm{sgn}(p)\cos^{-1}\left[\frac{1-E}{\sqrt{E}}e^{\alpha(x-x_e)} - \frac{1}{\sqrt{E}}\right], \tag{5b}$$

are a convenient and natural representation to work with. In terms of (J,θ) the Hamiltonian in Eq. (1) can be written down as

$$H(J,\theta;t) = H_0(J) - \epsilon v(J,\theta;t), \tag{6}$$

with $\epsilon \equiv \lambda_1 d_1$ and

$$H_0(J) = \omega_0\left(J - \frac{\omega_0}{4D_0}J^2\right),$$

$$v(J,\theta;t) = 2\left[V_0(J) + \sum_{n=1}^{\infty} V_n(J)\cos(n\theta)\right]\cos(\omega_F t), \tag{7}$$

being the zeroth-order (matter) Hamiltonian and the interaction with the field, respectively. In the above equations, $E = H_0/D_0 < 1$ denotes the dimensionless bound state energy, $\omega_0 = (2\alpha^2 D_0/M)^{1/2}$ is the harmonic frequency, and $\mathrm{sgn}(p) = 1$ for $p \geq 0$, $\mathrm{sgn}(p) = -1$ for $p < 0$. The Fourier coefficients $V_0(J)$ and $V_n(J)$ are known analytically [16,47] and given by

$$V_0(J) = \frac{1}{4\alpha}\ln\left[\frac{D_0 + \sqrt{D_0^2 - D_0E(J)}}{2[D_0 - E(J)]}\right], \tag{8a}$$

$$V_n(J) = \frac{(-1)^{n+1}}{\alpha n}\left[\frac{\sqrt{D_0 E(J)}}{D_0 + \sqrt{D_0^2 - D_0 E(J)}}\right]^n. \quad (8b)$$

Note that the classical nonlinear frequency of the Morse oscillator is given by

$$\Omega_0(J) = \frac{\partial H_0}{\partial J} = \omega_0\left(1 - \frac{\omega_0}{2D_0}J\right). \quad (9)$$

We highlight and illustrate the central features of our work using the specific example of the hydrogen fluoride (HF) molecule [15]. Also, note that throughout this work we use atomic units for both the molecular and field parameters with time being measured in units of the field period $\tau_F = 2\pi/\omega_F$. Thus, we choose [15] $D_0 = 0.225, \alpha = 1.174, x_e = 1.7329$ and, $M = 1744.59$ corresponding to a total of $N_B = 24$ bound states supported by the Morse potential well. A fit [60] to the *ab initio* data on HF yields the following dipole function:

$$\mu(x) = Axe^{-\beta x^4}, \quad (10)$$

with $A = 0.4541$ and $\beta = 0.0064$. The dissociation dynamics is studied with a fixed driving laser field amplitude of $\lambda_1 = 0.0287$ (~ 30 TW/cm^2) implying a field of moderate intensity. Consistently, we use a linear approximation to $\mu(x)$ corresponding to $d_1 \approx 0.33$ [cf. Eq. (4)].

III. CLASSICAL AND QUANTUM DISSOCIATION DYNAMICS

Although one can choose different classes of initial states for the study, in this work the initial states are chosen to be the zeroth-order Morse eigenstates χ_ν given by Eq. (3). The initial states are time evolved on a grid using the well established split-operator method [61] involving the short-time propagator

$$\hat{U}(\Delta t) = \exp\left(-i\frac{\Delta t}{2\hbar}\hat{V}\right)\exp\left(-i\frac{\Delta t}{\hbar}\hat{T}\right)\exp\left(-i\frac{\Delta t}{2\hbar}\hat{V}\right), \quad (11)$$

with T and V denoting the kinetic and potential energy operators, respectively. The time step was set to $\Delta t = 5 \times 10^{-3}\tau$ to ensure convergence of the dissociation probabilities over the timescales of interest of about $500\tau_F$. As is usual, unphysical reflection at the grid boundaries is avoided by employing an optical potential [15,62]

$$V_{\text{opt}}(x) = -\frac{iV_0}{(1 + e^{[-(x-x^*)/\eta]})}, \quad (12)$$

with parameters (in atomic units) $V_0 = 0.02$, $\eta = 0.35$, and $x^* = 16.74$. The introduction of V_{opt} smoothly damps the outgoing wave function and does not modify the time evolution of the bound states. The quantum dissociation probability is then calculated as

$$P_D^q(\tau) = 1 - \sum_{\kappa=0}^{N_B} |\langle \chi_\kappa | \chi_\nu(\tau)\rangle|^2, \quad (13)$$

where N_B is the number of bound states.

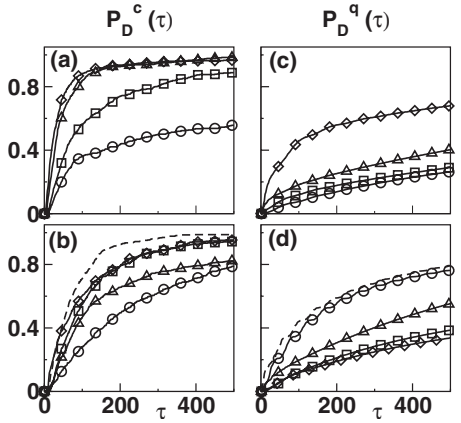

FIG. 1. Classical dissociation probabilities for the Morse oscillator states $\nu = 10$ (circles), 11 (squares), 12 (triangles), and 13 (diamonds) with driving field frequencies (in atomic units) (a) $\omega_F = 0.0129$ (b) 0.0178 and fixed field amplitude $\lambda_1 = 0.0287$ a.u. (~ 30 TW/cm^2). The corresponding quantum results are shown in the right column as (c) and (d), respectively. In case of $\omega_F = 0.0178$ an additional state $\nu = 14$ (dashed line) is also shown. Note that in this figure and all subsequent figures the various parameter values are in atomic units and time (τ) is measured in units of the field period, i.e., $\tau = t/\tau_F \equiv t(\omega_F/2\pi)$.

In order to compare and contrast the quantum dissociation dynamics with the classical dissociation dynamics we compute [63] the classical dissociation probabilities $P_C(\tau)$ by choosing an ensemble of initial trajectories N_{tot} with energy E_ν corresponding to the specific initial Morse state with the angle uniformly distributed in $[-\pi, \pi]$. During the time evolution, a trajectory is considered to be dissociated when the compensated energy

$$E_c \equiv \frac{1}{2M}\left[p - \frac{\epsilon}{\omega_F}\sin(\omega_F\tau)\right]^2 + D_0[1 - e^{-\alpha(x-x_e)}]^2 \quad (14)$$

exceeds the Morse dissociation energy D_0. The number of dissociated trajectories N_{dis} at a given time is determined from the above criteria and the resulting classical dissociation probability is the fraction

$$P_D^c(\tau) = \frac{N_{\text{dis}}}{N_{\text{tot}}}. \quad (15)$$

In Fig. 1 we show P_D^c and P_D^q as a function of time for some of the high-lying Morse eigenstates for two specific driving field frequencies (in atomic units) of $\omega_F = 0.0129$ and 0.0178. In particular note that, given the specific Morse parameters, $\omega_F = 0.0129$ is not resonant with the transition frequency between any of the states of interest in Fig. 1 and hence represents an off-resonant situation. However, $\omega_F = 0.0178$ is involved in a resonance with two of the states shown in Fig. 1 (specifically, $E_{14} - E_{10} \approx 2\hbar\omega_F$) and hence characterized as a two-photon resonant case. These cases, which will be used to highlight the results, are selected since they represent two limits in which classical-quantum correspondence either holds (off-resonant) or does not hold (on-resonant).

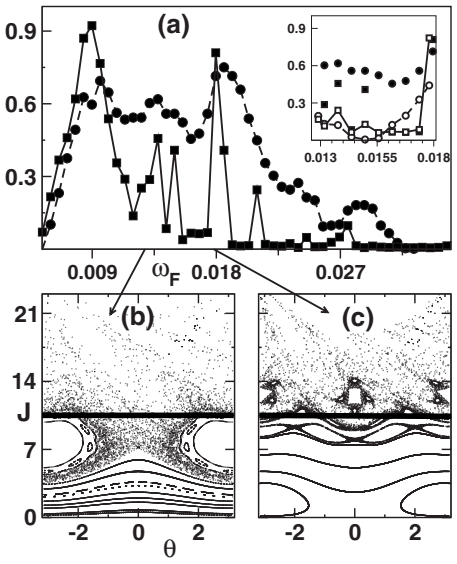

FIG. 2. (a) Quantum (filled squares, solid line) and classical (filled circles, dashed line) dissociation probabilities (y axis) for the Morse eigenstate $\nu=10$ of HF as a function of the field frequency ω_F (in atomic units). Note that the probabilities shown correspond to the final time $500\tau_F$ with fixed field strength $\lambda_1=0.0287$ a.u. Panels (b) and (c) show the stroboscopic surface of section for the two representative ω_F cases (indicated by arrows) considered in this work with $\omega_F=0.0129$ and 0.0178, respectively. The thick black lines in (b) and (c) are at the classical action value $J=10.5$ corresponding to quantum initial state $\nu=10$. The inset in (a) shows the control of $\nu=10$ dissociation, over the range $\omega_F \in (0.0128, 0.0178)$, by building the $1+\gamma^{-1}$ cantorus barrier in the classical (open circles, dashed line) and quantum (open squares, solid line) cases. The uncontrolled cases [filled symbols as in (a)] are also shown for comparison.

A comparison of the classical [Fig. 1(a)] and quantum [Fig. 1(c)] results in the off-resonant case reveals that the dissociation probabilities monotonically increase with increasing vibrational excitation. However, P_D^q is considerably smaller as compared to P_D^c. The reasons for this are well known and can be explained based on the classical phase space shown in Fig. 2(b). Extensive classical stickiness [63] around the initial action $J=10.5$ (corresponding to the quantum initial state $\nu=10$) leads to the reduced P_D^c for this state. At the same time the density variation in the chaotic regions of the phase space is symptomatic of the existence of partial barriers-in this case corresponding to a cantorus with $\omega_F/\Omega_0(J)=1+\gamma^{-1}$ with $\gamma\equiv(\sqrt{5}+1)/2\approx 1.618$ being the golden mean. Based on earlier works [15,47], it is reasonable to surmise that the quantum dissociation is blocked by the cantorus. On the other hand, dissociation probabilities for the on-resonant case shown in Figs. 1(b) and 1(d) indicate nontrivial behavior as compared to the off-resonant case. The quantum dissociation probabilities are nonmonotonic with initial states $\nu=10, 14$, having nearly identical P_D^q, dissociating far more than the state $\nu=13$. Quantum mechanically, resonant two-photon transition of state $\nu=10$ to $\nu=14$ leads to direct coupling with the continuum and hence enhances the dissociation of state $\nu=10$. The state-to-state transition probabilities indicate [15], not shown here, Rabi cycling between the states $\nu=10$, 12, and 14. Insights into such behavior can also be gained by studying the classical phase space structures as seen in Fig. 2(c). In this on-resonant case $J=10.5$ is essentially located around the $1+\gamma^{-1}$ cantorus and a prominent $\omega_F/\Omega_0(J)=2/1$ nonlinear resonance is observed. Clearly, the 2:1 resonance is the classical analog of the quantum two-photon resonance and must be playing a crucial role in the observed dissociation dynamics [17]. In the subsequent sections we will highlight the classical-quantum correspondence for both the off-resonant and on-resonant cases.

In order to illustrate the key features of this work we focus on the dissociation dynamics of the Morse state $\nu=10$ for the above mentioned field frequencies. The analysis, however, can be performed for any initial state and our specific choice is inspired by the earlier work of Brown and Wyatt [15]. Moreover, for moderate field intensities, state $\nu=10$ is an ideal choice to illustrate the interplay between classical and quantum dissociation mechanisms. Figure 2(a) provides the comparison of quantum and classical dissociation probabilities for $\nu=10$ interacting with a field with fixed intensity and for varying choice of the field frequencies ω_F. The quantum distribution exhibits peaks at certain frequencies corresponding to resonant multiphoton transitions. The classical dissociation profile rises with ω_F, broadens and dies out smoothly at higher frequencies due to the transition from trapping of trajectories in KAM tori at low frequencies to trapping inside the resonance island regions at higher frequencies. These observations are rather general and a detailed interpretation has been given earlier by Nicolaides and co-workers [63].

We now pose several questions in the context of Fig. 2. Is it possible to correlate the changes in classical phase space structures with the quantum dissociation probabilities in both off-resonant and on-resonant cases? What is the role, if any, of the classical nonlinear resonances in regulating the decay of quantum states? Finally, and the main focus of this work, can one control the classical and quantum dissociation dynamics by creating suitable local barriers in the classical phase space? For the present system the answer is in the affirmative and, as a preview to the rest of the paper, the inset to Fig. 2(a) shows the suppression of classical and quantum dissociation by locally creating a cantorus with winding number $\omega_F/\Omega_0(J)=1+\gamma^{-1}$. We now turn to the issue of local phase space control of dissociation which, as seen later, provides answers to the first two questions posed above as well.

IV. CONTROL BY REBUILDING A KAM TORUS

The phase spaces shown in Figs. 2(b) and 2(c), and the discussion in the previous section, suggest that if one can rebuild some of the irrational tori, such as the $1+\gamma^{-1}$ cantorus, locally in the phase space then it ought to be possible to suppress the dissociation. Given the close parallels between the atomic ionization and the system of interest to us, i.e., molecular dissociation, we employ the same classical perturbation theory approach [53] to obtain an analytic expression for the control field in case of the driven Morse oscillator. Since the technique has been described in consid-

erable detail in the earlier works [54,53], in what follows we provide the main results which are of relevance in the present context. In addition, note that we use the notation of Huang *et al.* for convenience as well as uniformity.

A. Methodology

To start with, the nonautonomous Hamiltonian is mapped into an autonomous one by considering $[t(\mathrm{mod}\, 2\pi), E]$ as an additional angle-action pair. Denoting the action and angle variables by $\mathbf{A} \equiv (J, E)$ and $\boldsymbol{\theta} \equiv (\theta, t)$ we can write the original driven system Hamiltonian [see Eq. (6)] as

$$H(\mathbf{A}, \boldsymbol{\theta}) = H_0(\mathbf{A}) - \epsilon V(\mathbf{A}, \boldsymbol{\theta}), \tag{16}$$

where we have denoted $V(\mathbf{A}, \boldsymbol{\theta}) \equiv v(J, \theta; t)$. Note that for a fixed driving field strength λ_1 and the value of d_1 corresponding to the HF molecule, $\epsilon \equiv \lambda_1 d_1$ is also fixed. Moreover, for physically meaningful values of d_1 for most diatomics and typical field strengths far below the ionization threshold one always has $\epsilon \ll 1$ ($\epsilon \sim 0.01$ in the present study). In the absence of the driving field ($\epsilon = 0$), the zeroth-order Hamiltonian is integrable and the phase space is foliated with invariant tori labeled by the action $\mathbf{A}$ corresponding to the frequency $\boldsymbol{\omega} \equiv \partial H_0 / \partial \mathbf{A} = (\Omega_0, \omega_F)$. However, in the presence of the driving field ($\epsilon \neq 0$) the field-matter interaction renders the system nonintegrable with a mixed regular-chaotic phase space. More specifically, for field strengths near or above a critical value ϵ_c one generally observes a large scale destruction of the field-free invariant tori leading to significant chaos and hence the onset of dissociation. The critical value ϵ_c itself is clearly dependent on the specific molecule and the initial state of interest. We remark here that the fixed value of the field strength, and hence ϵ, chosen for the present study is above the critical ϵ_c for the states of interest (shown in Fig. 1).

The aim of the local control method is to rebuild a nonresonant torus $\mathbf{A}_0 = (J_0, 0)$, $\mathbf{k} \cdot \boldsymbol{\omega} \neq 0$ with integer $\mathbf{k}$, which has been destroyed due to the interaction with the field. Assuming that the destruction of $\mathbf{A}_0$ is responsible for the significant dissociation observed for some initial state of interest, the hope is that locally recreating the $\mathbf{A}_0$ will suppress the dissociation, i.e., $\mathbf{A}_0$ acts as a local barrier to dissociation. Ideally, one would like to recreate the local barrier by using a second field (appropriately called as the control field) which is much weaker and distinct from the primary driving field. Following Huang *et al.* such a control field $f(\theta)$ can be obtained and has the form

$$f(\boldsymbol{\theta}) = -H[\mathbf{A}_0 - \partial_{\boldsymbol{\theta}} \Gamma b(\boldsymbol{\theta}), \boldsymbol{\theta}], \tag{17}$$

where $b(\boldsymbol{\theta}) \equiv H(\mathbf{A}_0, \theta) = \Sigma_{\mathbf{k}} b_{\mathbf{k}} e^{i\mathbf{k}\cdot\boldsymbol{\theta}}$ and Γ being a linear operator defined by

$$\Gamma b(\boldsymbol{\theta}) = \sum_{\mathbf{k}\cdot\boldsymbol{\omega} \neq 0} \frac{b_{\mathbf{k}}}{i\mathbf{k} \cdot \boldsymbol{\omega}} e^{i\mathbf{k}\cdot\boldsymbol{\theta}}. \tag{18}$$

The classical control Hamiltonian can now be written down as

$$H_c(\mathbf{A}, \boldsymbol{\theta}) = H(\mathbf{A}, \boldsymbol{\theta}) + f(\boldsymbol{\theta}) \equiv H_0(\mathbf{A}) - \epsilon V(\mathbf{A}, \boldsymbol{\theta}) + f(\boldsymbol{\theta}) \tag{19}$$

and below we show that the control term $f(\boldsymbol{\theta})$ is $O(\epsilon^2)$ to leading order. Since $1 \gg \epsilon > \epsilon_c$, the control term is indeed weaker than the primary driving field.

The control term can be explicitly derived for the Morse oscillator since the Fourier coefficients [cf. Eq. (8)] are known analytically. In addition, as we are focusing on the dissociation dynamics of the initial Morse oscillator state $\nu = 10$, a look at the phase spaces shown in Figs. 2(b) and 2(c) suggests the appropriate local barriers that need to be recreated. Referring to Figs. 2(b) and 2(c) it is clear that the classical action corresponding to the quantum initial state $\nu = 10$ is located between the primary resonances $\omega_F : \Omega_0 = 1:1$ and 2:1. Thus, in our case the aim is to try and rebuild tori with irrational frequency ratios between the two resonances. In particular, the golden mean tori ($1 + \gamma^{-n}$, integer n) are of specific interest in the driven Morse system [15,47]. In the absence of the primary driving field, such an invariant torus with frequency $\Omega_0 = \Omega_r$ is located at $J_r = (\omega_0 - \Omega_r)(2D_0/\omega_0^2)$. We shift the action $\tilde{J} = J - J_r$ to focus on the specific region of the phase space and expand the autonomous Hamiltonian to second order (exact for the Morse oscillator) in $\tilde{J}$. Following the methodology outlined above the control term is obtained as

$$f(\boldsymbol{\theta}) \equiv f(\theta, t) = \epsilon^2 \left\{ \frac{\omega_0^2}{4D_0} [\partial_\theta \Gamma b(\boldsymbol{\theta})]^2 + 2C_0(\boldsymbol{\theta}) + C_1(\boldsymbol{\theta}) \right\}, \tag{20}$$

where we have denoted

$$C_0(\boldsymbol{\theta}) \equiv \sum_{k=1}^{\infty} \frac{(-1)^k}{k!} \epsilon^{k-1} V_{0k}(J_r) (\partial_\theta \Gamma b)^k (\cos\, \omega_F t),$$

$$C_1(\boldsymbol{\theta}) \equiv \sum_{n=1}^{\infty} \left\{ \sum_{k=1}^{\infty} \frac{(-1)^k}{k!} \epsilon^{k-1} V_{nk}(J_r) (\partial_\theta \Gamma b)^k \right\} [\cos(n\theta + \omega_F t) + \cos(n\theta - \omega_F t)], \tag{21}$$

with

$$V_{nk}(J_r) \equiv \left(\frac{d^k}{d\tilde{J}^k} V_n(\tilde{J} + J_r) \right)_{\tilde{J}=0},$$

$$\Gamma \partial_\theta b(\boldsymbol{\theta}) = \partial_\theta \Gamma b(\boldsymbol{\theta}) = -\sum_{n=1}^{\infty} n V_n(J_r) \left[\frac{\cos(n\theta + \omega_F t)}{(n\Omega_r + \omega_F)} + \frac{\cos(n\theta - \omega_F t)}{(n\Omega_r - \omega_F)} \right]. \tag{22}$$

It is important to note that the full control field $f(\boldsymbol{\theta})$, given by Eq. (20), is $O(\epsilon^2)$ to leading order as discussed earlier and hence weaker than the primary driving field. Since we are in a regime corresponding to $\epsilon \ll 1$ it is sufficient to retain the $O(\epsilon^2)$ term in Eq. (20) and, as a consequence, the full control Hamiltonian can be approximated as

$$H(J,\theta;t) = H_0(J) - \epsilon v(J,\theta;t) + f(\theta,t)$$
$$\approx H_0(J) - \epsilon v(J,\theta;t) + \epsilon^2 g_a(\theta,t), \quad (23)$$

where we have denoted

$$g_a(\theta,t) = \left\{ \frac{\omega_0^2}{4D_0}(\partial_\theta \Gamma b)^2 - 2V_{01}(\partial_\theta \Gamma b)\cos(\omega_F t) - (\partial_\theta \Gamma b)\zeta(J,\theta;t) \right\}, \quad (24)$$

and it can be shown that

$$V_{01} = \frac{\omega_0^2}{8\alpha\Omega_r D_0}\left(\frac{2\omega_0 + \Omega_r}{\omega_0 + \Omega_r}\right),$$

$$V_{n1} = (-1)^{n+1}\left(\frac{\omega_0^3}{2\alpha D_0}\right)\frac{(\omega_0 - \Omega_r)^{n/2-1}}{(\omega_0 + \Omega_r)^{n/2+1}},$$

$$\zeta(J,\theta;t) = \sum_{n=1}^{\infty} V_{n1}(J_r)[(\cos(n\theta + \omega_F t) + \cos(n\theta - \omega_F t)]. \quad (25)$$

As a remark we mention that the perturbative treatment carried out to derive the control field $f(\theta,t)$ breaks down when $n\Omega_r \approx \omega_F$. Thus, assuming a nonresonant Ω_r, the recreated torus to $O(\epsilon)$ is located at

$$J(\boldsymbol{\theta}) = J_r - \epsilon\partial_\theta \Gamma b. \quad (26)$$

B. Simplifying the control term

The control fields $f(\boldsymbol{\theta})$ and $f_a(\boldsymbol{\theta}) \equiv \epsilon^2 g_a(\boldsymbol{\theta})$ obtained above can be used for studying the control of classical dissociation dynamics. However, a direct use of the control terms in quantum studies is subtle since the notion of action-angle variables does not exist except in the semiclassical limit. Moreover, transforming back even the leading order control term $f_a(\boldsymbol{\theta})$ to the original (x,p,t) variables via the canonical transformations in Eq. (5) is difficult. In any case, at the quantum level one would face the usual xp-ordering issues in order to have the proper quantum control Hamiltonian. Thus, in order to implement the classical control terms for studying their effect on the quantum dissociation dynamics it is necessary to simplify the form of the control field. Fortunately, Huang *et al.* [53] have already suggested such a simplification and we briefly outline their approach.

The control term being periodic in θ and t has a rich Fourier spectrum. However, only few of the Fourier components are dominant and the parameter

$$G_{k_1,k_2} \equiv \frac{|F_{k_1,k_2}|}{|k_1\Omega_r + k_2\omega_F|}, \quad (27)$$

with F_{k_1,k_2} being the coefficients in the double Fourier expansion of the control term f or f_a is used to identify those dominant modes. Note that this implies large amplitude F_{k_1,k_2} and $k_1\Omega_r + k_2\omega_F \approx 0$ i.e., the corresponding wave vector is close to being in resonance with the frequency vector $\boldsymbol{\omega}$ of the integrable motion. Once identified, only the dominant Fourier modes are retained in the control term. Further simplification, required for quantum studies, is obtained by mapping a typical dominant term as

$$F_{k_1,k_2}\cos(k_1\theta + k_2\omega_F t) \rightarrow \lambda_2(k_1,k_2)\cos(k_2\omega_F t). \quad (28)$$

The coefficients $\lambda_2(k_1,k_2)$ are determined [53] by comparing the dominant Fourier mode amplitudes in the original control Hamiltonian with the corresponding amplitudes in the simplified control Hamiltonian

$$H_c = H(J,\theta;t) + \mu(x)\lambda_2(k_1,k_2)\cos(k_2\omega_F t). \quad (29)$$

If more than one dominant Fourier modes are present then they will appear as additional terms in Eq. (29). For all the results presented in the next few sections we have used the control Hamiltonian of the form given above.

V. INFLUENCE OF THE CONTROL FIELD ON DISSOCIATION DYNAMICS

We now present our results for the effect of local phase space barriers on the dissociation dynamics of the Morse state $\nu = 10$ for the two representative field frequencies and compare to the uncontrolled results summarized in Figs. 1 and 2. As we are interested in understanding the effect of creating cantori barriers on both the classical and quantum dynamics we also show, following earlier studies on quantum transport through cantori [46,64,65], the time-averaged probability

$$P_{\nu,\nu'} = \lim_{T\rightarrow\infty}\frac{1}{T}\int_0^T d\tau|\langle\chi_{\nu'}|\chi_\nu(\tau)\rangle|^2, \quad (30)$$

of being in a state $\chi_{\nu'}$ having started in the initial state χ_ν. In this work $T = 500\tau_F$ is a sufficiently long time for computing $P_{\nu,\nu'}$. The classical analog of Eq. (30) is constructed by coarse-graining the actions, i.e., the trajectory is considered to be in the action region J if it is located within a bin of width 0.5 centered about J. Reasonable variations of the bin width lead to qualitatively similar results and convergence can be easily checked. Such a coarse-graining procedure is appropriate for studying the classical-quantum correspondence of $P_{\nu,\nu'}$.

A. Off-resonant laser field

Figure 3 summarizes our results for the off-resonant case with two different cantori barriers being rebuilt in the phase space. These cantori, corresponding to $\omega_F/\Omega_r = 1 + \gamma^{-1}$ (shown in red/dark gray), and $1 + \gamma^{-2}$ (shown in green/light gray), are located at actions $J_r \approx 13.8$ and 12.0, respectively. The modified (θ,J) phase spaces shown in Figs. 3(c) and 3(d) clearly show the reconstruction of the respective barriers as evidenced by the reduction of stochasticity and increased stickiness around the regular regions. These phase spaces should be compared to the one shown in Fig. 2(b) corresponding to the uncontrolled phase space. Importantly, and as anticipated from the discussions in Sec. IV, the control fields are indeed weaker than the primary driving field

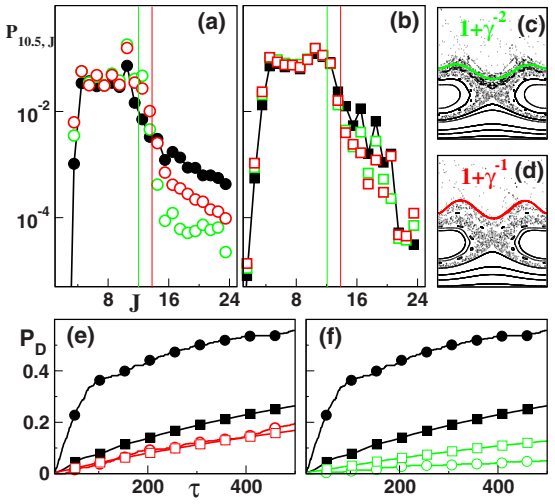

FIG. 3. (Color online) This figure summarizes the result of creating two local phase space barriers $\omega_F/\Omega(J)=1+\gamma^{-1}$ and $\omega_F/\Omega(J)=1+\gamma^{-2}$ on the classical and quantum dynamics for $\omega_F=0.0129$ a.u. (off-resonance) and initial state $\nu=10$. The recreated barriers effectively reduce the extent of chaos, as compared to Fig. 2(b), and evident from the (θ,J) phase spaces shown in (c) $\omega_F/\Omega(J)=1+\gamma^{-2}$ and (d) $\omega_F/\Omega(J)=1+\gamma^{-1}$. Note that (c) and (d) have identical axes range as in Fig. 2(b) and the perturbatively recreated tori, $1+\gamma^{-1}$ in red/dark gray, and $1+\gamma^{-2}$ in green/light gray, according to Eq. (26) are also shown. (a) Classical time-averaged ($T=500\tau_F$) cross probabilities $P_{\nu,\nu'}$ [cf. Eq. (30)] as a function of $J=\nu'+1/2$ for the uncontrolled (filled circles), controlled ($1+\gamma^{-1}$, red/dark gray open circles), and controlled ($1+\gamma^{-2}$, green/light-gray open circles) showing the influence of the recreated barriers. (b) Same as in (a) showing the quantum time-averaged ($T=500\tau_F$) cross probabilities $P_{\nu,\nu'}$ (squares) versus J. The thin vertical lines in (a) and (b) show the expected location of the recreated ($1+\gamma^{-1}$ in red and $1+\gamma^{-2}$ in green/light gray) KAM barriers. In (e) and (f) the dissociation probabilities, with colors and symbols as in (a) and (b), are shown as a function of time and correspond to cases (d) and (c), respectively. See text for discussion.

strength. This is confirmed in Figs. 4(a)–4(c) where we compare the primary driving field with frequency $\omega_F=0.0129$, the full control term given by Eq. (20), and the leading order control term of Eq. (24), respectively, as a function of θ and τ. It is clear that not only are the control fields weaker by an order of magnitude but the leading order approximation to the full control term is fairly good. Furthermore, in Fig. 4(d) we show the result of Fourier transforming the leading order term $f_a(\boldsymbol{\theta})$ via the parameter G_{k_1,k_2}, defined in Eq. (27), in order to obtain a simplified control field. One finds a single dominant Fourier mode with $(k_1,k_2)=(3,-2)$ with $\lambda_2\approx 0.017$. In other words the control field is of the form $\lambda_2\cos(2\omega_F t)$ $(=\lambda_2\cos(4\pi\tau)$ since t is in units of the field period τ_F) and, since $\lambda_2>0$, comes with a phase difference of π relative to the driving field. Figure 4(e) shows that the simplified control field is not just an out of phase contribution that acts to reduce the primary driving field strength below the critical threshold for dissociation. Note that the same dominant Fourier mode is observed (not shown) in case of the control field used to create the $1+\gamma^{-2}$ barrier and yields $\lambda_2\approx 0.011$. We remark at this juncture that the simplified control fields, for example as shown in Fig. 4(e), in both cases have strengths which are a factor of 2–3 weaker than the primary driving field. This is in contrast to the full or leading order classical control fields which are nearly an order of magnitude smaller as seen in Figs. 4(b) and 4(c). This is clearly due to the fact that we are approximating the classical control field as $f_a(\theta,t)\approx\lambda_2(k_1,k_2)\cos(k_2\omega_F t)$ in order to obtain the simplified control field. Nevertheless, it is crucial to observe that the simplified control fields are weaker than the primary driving field and, in particular, Figs. 3(c) and 3(f) show that the dissociation can be suppressed substantially by an even weaker simplified control field corresponding to recreating the $1+\gamma^{-2}$ barrier. Interestingly, Wu *et al.* [27] in an earlier work have suggested precisely the same control field characteristics for suppressing chaos in the driven Morse system. However, they were not clear about the mechanism for the suppression and this work yields the necessary insight in terms of the creation of local cantori barriers.

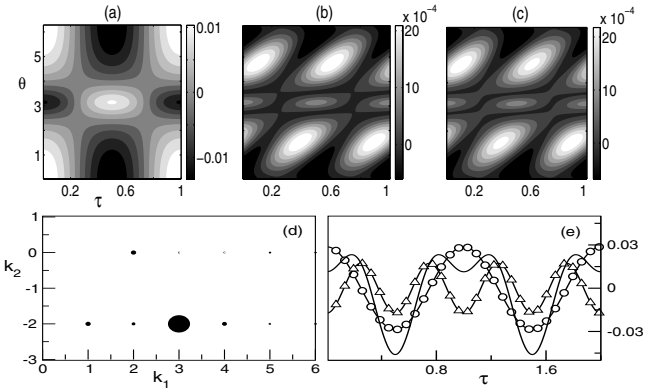

FIG. 4. (a) Primary driving field $\epsilon v(J_r,\theta;t)$ with frequency $\omega_F=0.0129$ a.u. corresponding to the off-resonant case. (b) Control field given by Eq. (20) designed to recreate the $\omega_F/\Omega_r=1+\gamma^{-1}$ tori located at $J_r\approx 13.8$. (c) Leading order approximation to (b) given by Eq. (24). Note that the classical control fields in (b) and (c) are an order of magnitude smaller as compared to the primary field in (a). In (d) the parameter G_{k_1,k_2} as defined in Eq. (27) shows the dominance (via circles with varying sizes) of the $(k_1,k_2)=(3,-2)$ Fourier mode. (e) The simplified control field [$\lambda_2\cos(4\pi\tau+\pi)$, triangles] [see Eq. (29)] and the primary driving field [$\lambda_1\cos(2\pi\tau)$, circles] as a function of time $\tau\equiv t/\tau_F$ in units of the primary field period τ_F. The sum of the driving field and the simplified control field is also shown as a line (no symbols). Note that the simplified control field is roughly a factor of 2 weaker as compared to the driving field, in contrast to those shown in (b) and (c). See text for discussion.

For further insights into the role and efficiency of the cantori barriers toward controlling the dissociation dynamics, in Figs. 3(a) and 3(b) the classical and quantum time-averaged probabilities $P_{\nu,\nu'}$ defined in Eq. (30) are shown. Also shown in these figures are the approximate locations of the cantori as thin vertical lines at the corresponding action values $J=J_r$. The classical $P_{\nu,\nu'}$ in Fig. 3(a) show that the probabilities fall rapidly in the vicinity of the rebuilt cantori, especially in case of the $1+\gamma^{-2}$ cantorus. Consequently, dramatic reduction in the classical dissociation probability in both the cases can be seen (circles) from Figs. 3(e) and 3(f). It is possible to investigate more detailed aspects of the clas-

sical phase space transport across the cantori, as done for other systems [64,65], but we do not pursue them in this work. Moreover, it is known that the driven Morse oscillator dynamics near the separatrix can be analyzed from the perspective of a whisker map for which Maitra and Heller [65] have already provided a detailed classical-quantum correspondence of the transport across cantori.

A key issue that we are interested in this paper is whether the quantum dissociation is sensitive to the classical phase space barriers being rebuilt. Note that all the quantum calculations performed herein have $\hbar=1$ and hence we are in the "quantum regime." Therefore, *a priori* one might anticipate that quantum effects can override or ignore the changes in the classical phase space. However, in this off-resonant case, we see from Figs. 3(e) and 3(f) that the quantum results (squares) exhibit clear reduction in the dissociation probabilities [see inset to Fig. 2(a) for the entire range of field frequency]. Analogous to the classical case, the $1+\gamma^{-2}$ cantorus is a stronger barrier to dissociation as seen by comparing Fig. 3(e) with Fig. 3(f). The quantum time-averaged probability $P_{\nu,\nu'}$ is shown in Fig. 3(b) and exhibits the expected suppression of probabilities for states lying around and beyond the location of the classical cantori. Comparing the quantum $P_{\nu,\nu'}$ with the classical results shown in Fig. 3(a) we make a few important observations. First, the finite probabilities for low lying Morse states ($\nu \leq 4$) seen in the quantum $P_{\nu,\nu'}$ are strictly zero in the classical case. This is due to dynamical tunneling through the classical KAM barriers as proposed nearly two decades ago by Davis and Wyatt [14]. Second, the quantum results exhibit oscillations beyond the cantori barrier in contrast to the smooth classical decay. We suggest that this is a manifestation of what Maitra and Heller called "retunneling" in their study [65] of the whisker map. Although the reconstructed cantori are perceived as complete barriers by the quantum system, some of the quantum states are able to tunnel efficiently across the cantori since $\hbar$ is large, i.e., the quantum mechanism (enhancement due to tunneling) dominates the classical (suppression due to cantorus) mechanism. This might explain as to why the suppression of quantum dissociation probability due to the $1+\gamma^{-1}$ barrier is not significantly different from that due to the $1+\gamma^{-2}$ barrier in contrast to the classical results.

Despite the comments made above, it is clear from Fig. 3 that the classical-quantum correspondence holds for local phase space control in the off-resonance case. We now discuss the on-resonant case wherein such a correspondence is not expected to hold.

B. On-resonance laser field

As mentioned in Sec. III, with the primary driving field frequency value of $\omega_F=0.0178$ the quantum system is in the two-photon resonant regime involving the Morse states $\nu=10$, 12, and 14. This is reflected in the quantum dissociation probabilities shown in Fig. 1(d) as well as in the classical phase space as a large 2:1 nonlinear resonance zone [cf. Fig. 2(b)]. Importance of this resonance, embedded in the chaotic region between the unperturbed $1+\gamma^{-1}$ and $2+\gamma^{-1}$ cantori, was noted by Brown and Wyatt [15] as well as Dardi and

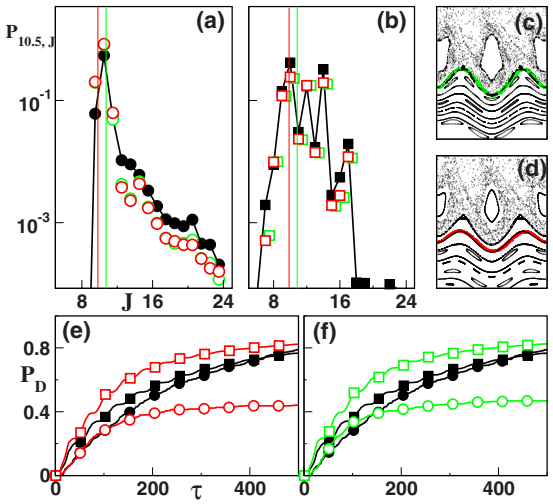

FIG. 5. (Color online) Results for initial state $\nu=10$ in the on-resonant case $\omega_F=0.0178$ a.u., with same notations as in Fig. 3, showing the effect of creating local barriers $\omega_F/\Omega(J)\approx\sqrt{3}$ (green/light gray) and $\omega_F/\Omega(J)=1+\gamma^{-1}$ (red/dark gray). The respective (θ,J) phase spaces near the 2:1 resonance are shown in (c) and (d). In (c) and (d) the angle $\theta\in(-\pi,\pi)$ but the action $J\in(6,16.5)$. As in Fig. 3, the comparison of the uncontrolled and controlled dissociation probabilities for cases (c) and (d) are shown in (f) and (e), respectively. Note that in this figure the results corresponding to $\omega_F/\Omega(J)\approx\sqrt{3}$ are obtained by retaining the $(3,-2)$ Fourier mode alone. See the discussion following Eq. (31) and Fig. 6 for details.

Gray [17] in an earlier work. Indeed, our computations (not shown here) indicate that the Wigner function of state $\nu=12$ is localized on the resonance with the Wigner functions associated with $\nu=10$ and 14 straddling the resonance zone. Such a situation is tailor made for the manifestation of resonance-assisted tunneling in the system [47,56–58]. Combined with the observation that the initial state of interest is located right around the $1+\gamma^{-1}$ cantorus [see Fig. 2(c)], one expects significant competition between the quantum and classical mechanisms for dissociation. Consequently, the two-photon case provides a difficult challenge for the local phase space control method.

In Fig. 5 we summarize the results of our attempts to control the dissociation by creating the local barriers with $\omega_F/\Omega_r\approx\sqrt{3}$ (green/light gray) and $\omega_F/\Omega_r=1+\gamma^{-1}$ (red/dark gray). We did not attempt to create the $1+\gamma^{-2}$ barrier since it would be located much below the action ($J=10.5$) of the initial state in the classical phase space. Results for the two cases will be discussed separately in order to illustrate the interplay between classical and quantum dissociation mechanisms. Moreover, in the $\omega_F/\Omega_r\approx\sqrt{3}$ case, complications arise in determining the simplified control Hamiltonian which requires additional discussion.

Since Fig. 2(c) shows that the initial state is located in the region corresponding to the $1+\gamma^{-1}$ cantorus we attempt to rebuild the cantorus and Fig. 5(d) shows that the attempt is successful. The simplified control field in Eq. (29) is of the form $\lambda_2\cos(2\omega_F t)$, corresponding to the dominant Fourier mode $F_{3,-2}$, with $\lambda_2\approx 0.008$ and hence, as in the previous off-resonance case comes with a relative phase of π. Robust barriers have been created in the phase space with a local

control field strength λ_2 which is nearly four times weaker than the driving field strength. The time-averaged probabilities in Fig. 5(a) exhibit rapid decay in the vicinity of the recreated barrier and the classical dissociation probability, shown in Fig. 5(e), is reduced by nearly a factor of 2. Surprisingly enough, Fig. 5(e) shows that the quantum dissociation is *enhanced by a small amount* consistent with the behavior of the time-averaged probabilities shown in Fig. 5(b). The quantum result, in contrast to the off-resonance case, indicates that both classical and quantum mechanisms are at work in this instance.

On the other hand, attempts to create the $\omega_F/\Omega_r \approx \sqrt{3}$ barrier pose a problem, associated with the simplification of the control term Eq. (29), which was not encountered in the previous examples. Interestingly, in this case two dominant Fourier modes $F_{3,-2}$ and $F_{4,-2}$ are found with the corresponding values $G_{3,-2} \approx 0.029$ and $G_{4,-2} \approx 0.024$ [cf. Eq. (27)]. Taking into account only the marginally dominant $(3,-2)$ mode Fig. 5(c) shows that the desired local barrier is created. Consequently, Fig. 5(f) shows that the classical dissociation probability is, as in the case of the $1+\gamma^{-1}$ barrier, reduced by a factor of 2. Again one observes that the quantum counterpart behaves in an opposite manner, i.e., the dissociation is slightly enhanced. However, given that the Fourier mode $(4,-2)$ is nearly as dominant as the $(3,-2)$ mode, it seems reasonable to use an effective λ_2 in the simplified control term of Eq. (29) as

$$\lambda_2 = \frac{F_{3,-2}}{V_3(J_r)} + \frac{F_{4,-2}}{V_4(J_r)}. \tag{31}$$

Such a procedure yields $\lambda_2 \approx -0.015$ and thus the control field, still less intense than the primary field, comes with a relative phase of zero. Nevertheless, such an attempt fails as seen by inspecting the phase space shown in Fig. 6(c) which exhibits increased stochasticity and, expectedly, leads to enhanced classical dissociation observed in Fig. 6(d). Now, however, Fig. 6(e) shows that *the quantum dissociation is suppressed appreciably* and hence it would seem as if the quantum dynamics feels the barrier where there is none. Arguments invoking the large finite value of $\hbar$ and dynamical localization can be safely ignored since the phase space in Fig. 6(c) does not show any appreciable stickiness near the apparent barrier. The resolution to such an unexpected result comes from a closer inspection of the phase space in Fig. 6(c). One can clearly see that the attempt to create the local barrier has resulted in a severe perturbation of the 2:1 nonlinear resonance. As the additional Fourier mode $(4,-2)$ implies $2\Omega_r \approx \omega_F$, the observed perturbation can be tracked to the specific mode as long as it comes with an opposite phase. This will be established in the following subsection [cf. Eq. (38)]. Since this specific resonance is key to the two-photon process, it should not be surprising that the quantum dissociation is suppressed.

It is crucial to note that failure to create the barrier of interest occurs only when the control term is mapped to the simplified form as in Eq. (29) using the effective value for λ_2 shown above. This is confirmed by inspecting the phase spaces shown in Figs. 6(a) and 6(b) associated with the full

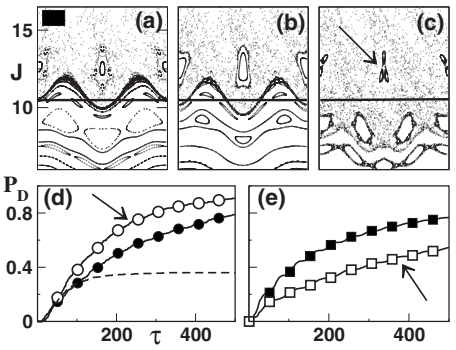

FIG. 6. Phase spaces (θ, J), with $\theta \in (-\pi, \pi)$ as x axis, corresponding to creating $\omega_F/\Omega(J) \approx \sqrt{3}$ barrier in the on-resonant case with (a) full leading order control term [cf. Eq. (24)], (b) retaining two dominant Fourier modes [cf. Eq. (32)], and (c) simplified control term [cf. Eq. (29)] using both Fourier modes and effective strength λ_2 obtained from Eq. (31). In (a) the size of the black square represents $\hbar = 1$. The rebuilt KAM torus can be clearly seen in (a) and (b) around the region $J = 10.5$ (thick line). However, in (c) it is clear that the intended barrier is not created. In (c) the perturbation of the 2:1 resonance is indicated by an arrow. Panel (d) shows the classical dissociation probabilities corresponding to (b) dashed line and (c) open circles as compared to the uncontrolled case (filled circles). Panel (e) shows the quantum dissociation probability corresponding to (c) open squares as compared to the uncontrolled case (filled squares).

$O(\epsilon^2)$ control Hamiltonian [see Eq. (24)] and the approximate Hamiltonian

$$H_c(J,\theta,t) \approx H(J,\theta,t) + \sum_{n=3,4} F_{n,-2} \cos(n\theta - 2\omega_F t), \tag{32}$$

obtained by retaining only the dominant Fourier modes in the control term. The recreated barriers in the phase space can now be clearly seen and Fig. 6(d) shows that the classical dissociation computed using the Hamiltonian in Eq. (32) is indeed suppressed. Clearly, the opposing classical and quantum results in this subsection, with the associated phase space structures, point to the importance of the quantum dissociation mechanism in the on-resonant case. In what follows we show that these observations can be rationalized based on the phenomenon of resonance-assisted tunneling.

1. Dissociation via resonance-assisted tunneling

In order to confirm the above arguments and to gain a better understanding of the results shown in Figs. 5 and 6 for the dissociation of the state $\nu = 10$ we focus on the role of 2:1 resonance within the paradigm of resonance-assisted tunneling. Following the earlier works [56–58], the motion in the vicinity of a $r:s$ resonance is analyzed by applying secular perturbation theory on the uncontrolled Hamiltonian in Eq. (6) and for details we refer the reader to the original work [56]. First, a canonical transformation to the appropriate slow angle $\theta \to \phi = \theta - \Omega_{r:s} t, J \to J$ is made resulting in the new Hamiltonian

$$\tilde{H}(J,\phi,t) = H_0(J) - \Omega_{r:s}J + \tilde{V}(J,\phi,t), \tag{33}$$

where $\tilde{V}(J,\phi,t)=V(J,\phi+\Omega_{r:s}t,t)$ and we have denoted $V(J,\theta,t)\equiv-\epsilon v(J,\theta;t)$ [cf. Eq. (8)]. We now expand H_0 in Eq. (33) about the resonant action $J_{r:s}$ to obtain the zeroth-order Hamiltonian in the vicinity of $r:s$ of the form

$$\tilde{H}_0(J) = \tilde{H}_0(J_{r:s}) + \frac{1}{2m_{r:s}}(\Delta J)^2, \tag{34}$$

with $\Delta J\equiv J-J_{r:s}$ and $m_{r:s}\equiv-2D_0/\omega_0^2$. Since, ϕ varies slowly near $r:s$, $\tilde{V}(J,\phi,t)$ is replaced by its average over r field periods

$$V_{\rm av}(J,\phi) \equiv \frac{1}{r\tau}\int_0^{r\tau}\tilde{V}(J,\phi,t)dt \simeq \lambda_1\sum_{n=1}^{\infty}V_n(J)\cos(nr\phi). \tag{35}$$

Ignoring the higher harmonics in the above expression and neglecting the action dependence of the Fourier coefficients V_n we obtain an effective (integrable) pendulum Hamiltonian

$$H_{\rm eff}(J,\phi) \simeq \frac{1}{2\tilde{m}_{r:s}}(\Delta J)^2 + 2\tilde{V}_{r:s}(J_{r:s})\cos(r\phi), \tag{36}$$

to describe the dynamics near the $r:s$ resonance with $\tilde{m}_{r:s}=-m_{r:s}$ and $V_{r:s}(J)=\epsilon V_1(J)/2$.

Specializing the above result to the observed 2:1 resonance, the resonant action is determined to be $J_{2:1}=12.6$, thus confirming the participation of the Morse state $\nu=12$. Using the zeroth-order Hamiltonian in Eq. (36) one finds, with $J=10.5$ (quantum state $\nu=10$) and $J'=14.5$ (quantum state $\nu'=14$), that

$$|E_J - E_{J'}| = \left|\frac{1}{2\tilde{m}_{2:1}}(J-J')(J+J'-2J_{2:1})\right| \approx 3.2\times10^{-4}, \tag{37}$$

i.e., the states $\nu=10$ and $\nu=14$ are nearly symmetrical with respect to the state $\nu=12$ localized on the 2:1 resonance [47,56]. Therefore, the nonzero coupling $V_{2:1}$ will efficiently connect the states $\nu=10$ and $\nu=14$. Moreover, it is possible to estimate the strength of the resonance for the given parameters as $V_{2:1}(J_{2:1})\approx0.01464$. It is crucial to note that the effective control field coupling strength from Eq. (31) in case of $\omega_F/\Omega_r\approx\sqrt{3}$, i.e., relevant to the phase space shown in Fig. 6(c) satisfies

$$\lambda_2 \approx -V_{2:1}(J_{2:1}). \tag{38}$$

Thus the control field with a zero relative phase tends to negate the effect of the 2:1 resonance generated by the primary driving field and this can be clearly seen in Fig. 6(c). We also remark here that the substantial quantum dissociation probability seen in Fig. 6(e), despite the strong perturbation of the 2:1 resonance, is due to the higher harmonics which have been neglected in the present analysis. This confirms our suspicion that the decay of state $\nu=10$ in the two-photon regime is dominated by resonance-assisted tunneling.

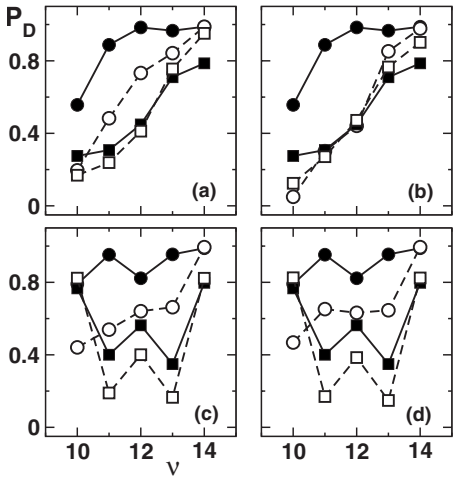

FIG. 7. Effect of the local barriers on the dissociation probability of nearby states, specified by ν, at $t=500\tau_F$. (a) and (b), with off-resonance $\omega_F=0.0129$ a.u., correspond to the creation of the $1+\gamma^{-1}$ and $1+\gamma^{-2}$ barriers, respectively. Panels (c) and (d), with on-resonance $\omega_F=0.0178$ a.u., correspond to the creation of the $1+\gamma^{-1}$ and $\sqrt{3}$ barriers, respectively, with fixed field strength as in the previous figures. The uncontrolled results are shown as filled symbols, classical (circles) and quantum (squares), while the controlled results are shown as corresponding open symbols. The lines are drawn as a guide for the eyes.

C. Are the rebuilt barriers local?

Up until now most of our results and discussions have focused on a specific initial Morse state. The barriers were created locally in phase space to influence the dissociation dynamics of the state $\nu=10$. From a control point of view, it is of some interest to examine the effect of such barriers on the dynamics of other states, especially states that are in the vicinity of state $\nu=10$. In other words, how local are these barriers? Toward this end, in Fig. 7 we show the influence of the local barriers on the dissociation probabilities of other nearby Morse states with $\nu>10$. At this stage it is useful to recall the results shown in Fig. 1 with the essential differences between the off-resonant and on-resonant cases. The effects of the $1+\gamma^{-1}$ and $1+\gamma^{-2}$ barriers in the off-resonant case, located around $J_r\approx13.8$ and 12.0, are shown in Figs. 7(a) and 7(b), respectively. These figures confirm that to a large extent the barriers are indeed local, i.e., dissociation is suppressed to varying extent for initial states lying below the barrier. For states lying above the barrier, dissociation is either enhanced (mostly in the quantum case) or slightly reduced.

On the other hand the quantum results for the on-resonant case, shown in Figs. 7(c) and 7(d) for the $1+\gamma^{-1}$ ($J_r\approx9.9$) and $\sqrt{3}$ ($J_r\approx10.9$) barriers [corresponding to Fig. 5(c), i.e., with only the $(3,-2)$ Fourier mode included] respectively, are far less straightforward to interpret. This is not entirely surprising since, as shown in the last section, resonance-assisted tunneling plays an important role and overrides the suppression due to the local barriers. In particular, the dissociation probabilities for states $\nu=10$ and $\nu=14$ increase very slightly. However, for the states $\nu=11$ and $\nu=13$, not involved in the resonance-assisted tunneling process, one ob-

serves substantially reduced dissociation despite being located far above the local barriers. We suspect that this is due to the increased stickiness around the 2:1 resonance region observed in the controlled phase spaces shown in Figs. 5(c) and 5(d). Note that this is corroborated by the observation that the concerned states also exhibit reduced classical dissociation as seen in Figs. 7(c) and 7(d). Further confirmation comes from our calculations which show an opposite quantum trend to that of Fig. 7(d) upon inclusion of the $(4,-2)$ Fourier mode as well resulting in the phase space shown in Fig. 6(c). It is possible to implicate, albeit indirectly, the local barriers with the observed suppression since creating the barriers leads to a more regular phase space, slightly increased size of the 2:1 resonance region, and therefore increased stickiness. Nevertheless, comparing the off-resonant and on-resonant cases shown in Fig. 7, it is evident that the effects of creating local phase space barriers can be far more subtle to interpret in the latter case.

VI. CONCLUSIONS

To summarize, this work demonstrates that it is possible to control the dissociation dynamics of a driven Morse oscillator by creating local phase space barriers. A clear understanding of the effect of cantori on both classical and quantum dissociation dynamics is obtained [see inset in Fig. 2(a) for example]. This work also highlights the essential difference between off-resonant and on-resonant dynamics with resonance-assisted tunneling playing a prime role in the latter case. Although local phase space barriers are very efficient in reducing the dissociation in the off-resonant case, the results in Figs. 5 and 6 suggest that controlling the quantum dissociation in the on-resonant regime can be achieved by using control fields which selectively perturb the appropriate nonlinear field-matter resonance. Similar observations have been made earlier in a different context [58] and further studies are required to establish a general criteria for controlling the multiphoton processes from the viewpoint of local modification of the phase space structures.

Several questions, however, remain to be addressed and we mention a few important ones. First, there is the issue of the effectiveness of the local barriers in systems with more than 2 degrees of freedom since the invariant tori do not have the correct dimensionality to partition the phase space. However, there are reasons to hope that even for systems with higher degrees of freedom the rebuilt tori can act as barriers for short times [66]. A careful study of the classical and quantum transport with and without the control fields is required in this instance. Apart from polyatomic molecules, this is also important while considering the infrared multiphoton dissociation dynamics of a Morse oscillator by explicitly taking into account the rotations [67,68]. Second, one would like to extend the approach to systems under the influence of more general time-dependent fields, e.g., chirped fields. For slow chirping this should be feasible as one can then utilize the concept of adiabatic Floquet theory [69]. In case of arbitrary time-dependent fields the correct approach is not clear at the present moment. Third, the method used in the present and earlier works is dependent on our ability to express the Hamiltonian in terms of appropriate action-angle variables. This might pose some limitations which, as seen in the present work, can be more severe in terms of implementing the control into the quantum dynamics. Finally, for systems with small effective $\hbar$, the resonance-assisted tunneling mechanism will be replaced by chaos-assisted tunneling [70] and it would be interesting to study the influence of the cantori barriers in this context. These issues are the focus of ongoing work in our group.

ACKNOWLEDGMENTS

It is a pleasure to acknowledge useful discussions with Professor Cristel Chandre and Shu Huang on various aspects of local control theory. A.S. acknowledges financial support from University Grants Commission, India.

[1] P. M. Morse, Phys. Rev. **34**, 57 (1929).
[2] D. W. Lupo and M. Quack, Chem. Rev. **87**, 181 (1987).
[3] R. Marquardt and M. Quack, Infrared Phys. **29**, 485 (1989).
[4] J. Manz and G. K. Paramonov, J. Phys. Chem. **97**, 12625 (1993).
[5] A. A. Buchachenko and N. F. Stepanov, J. Chem. Phys. **98**, 5486 (1993).
[6] See, for example, B. Hartke, J. Manz, and J. Mathis, Chem. Phys. **139**, 123 (1989) and references therein.
[7] F. F. Crim, J. Phys. Chem. **100**, 12725 (1996).
[8] K. Bergmann, H. Theuer, and B. Shore, Rev. Mod. Phys. **70**, 1003 (1998).
[9] M. Shapiro and P. Brumer, *Principles of the Quantum Control of Molecular Processes* (Wiley, New York, 2003).
[10] S. A. Rice and M. Zhao, *Optical Control of Molecular Dynamics* (Wiley, New York, 2000).
[11] Y. Ohtsuki, M. Sugawara, H. Kono, and Y. Fujimura, Bull. Chem. Soc. Jpn. **74**, 1167 (2001).
[12] G. A. Voth and R. A. Marcus, J. Phys. Chem. **89**, 2208 (1985).
[13] R. B. Walker and R. K. Preston, J. Chem. Phys. **67**, 2017 (1977).
[14] M. J. Davis and R. E. Wyatt, Chem. Phys. Lett. **86**, 235 (1982).
[15] R. C. Brown and R. E. Wyatt, Phys. Rev. Lett. **57**, 1 (1986); R. C. Brown and R. E. Wyatt, J. Phys. Chem. **90**, 3590 (1986).
[16] M. E. Goggin and P. W. Milonni, Phys. Rev. A **37**, 796 (1988).
[17] P. S. Dardi and S. K. Gray, J. Chem. Phys. **77**, 1345 (1982); P. S. Dardi and S. K. Gray, *ibid.* **80**, 4738 (1984).
[18] S. K. Gray, Chem. Phys. **83**, 125 (1984).
[19] A. Guldberg and G. D. Billing, Chem. Phys. Lett. **186**, 229 (1991).
[20] J. J. Tanner and M. M. Maricq, Phys. Rev. A **40**, 4054 (1989).
[21] H.-P. Breuer and M. Holthaus, J. Phys. Chem. **97**, 12634 (1993).

[22] M. Thachuk and D. M. Wardlaw, J. Chem. Phys. **102**, 7462 (1995).
[23] M. E. Goggin and P. W. Milonni, Phys. Rev. A **38**, 5174 (1988).
[24] D. W. Noid and J. R. Stine, Chem. Phys. Lett. **65**, 153 (1979); J. R. Stine and D. W. Noid, Opt. Commun. **31**, 161 (1979).
[25] D. Beigie and S. Wiggins, Phys. Rev. A **45**, 4803 (1992).
[26] S. Chelkowski and A. D. Bandrauk, Chem. Phys. Lett. **233**, 185 (1995).
[27] Z. Wu, Z. Zhu, and C. Zhang, Phys. Rev. E **57**, 366 (1998).
[28] V. Constantoudis and C. A. Nicolaides, J. Chem. Phys. **122**, 084118 (2005).
[29] E. F. de Lima and M. A. M. de Aguiar, Phys. Rev. A **77**, 033406 (2008).
[30] S. Huang, C. Chandre, and T. Uzer, J. Chem. Phys. **128**, 174105 (2008).
[31] S. Chelkowski, A. D. Bandrauk, and P. B. Corkum, Phys. Rev. Lett. **65**, 2355 (1990).
[32] W. K. Liu, B. R. Wu, and J. M. Yuan, Phys. Rev. Lett. **75**, 1292 (1995); J. H. Kim, W. K. Liu, and J. M. Yuan, J. Chem. Phys. **111**, 216 (1999); J. H. Kim, W. K. Liu, F. R. W. McCourt, and J. M. Yuan, *ibid.* **112**, 1757 (2000).
[33] J. H. Kim and W. K. Liu, J. Chem. Phys. **111**, 216 (1999).
[34] H. Feng, Y. Liu, Y. Zheng, S. Ding, and W. Ren, Phys. Rev. A **75**, 063417 (2007); Y. Dai, Z. H. Geng, and S. L. Ding, *ibid.* **66**, 043415 (2002).
[35] B. D. Cahn and C. C. Martens, J. Chem. Phys. **99**, 7440 (1993).
[36] A. Kenfack and J. M. Rost, J. Chem. Phys. **123**, 204322 (2005); K. P. Singh, A. Kenfack, and J. M. Rost, Phys. Rev. A **77**, 022707 (2008); A. Kenfack, J. M. Rost, and F. Grossmann, N. J. Phys. **10**, 013020 (2008).
[37] See for example, C. M. Tesch, L. Kurtz, and R. de Vivie-Riedle, Chem. Phys. Lett. **343**, 633 (2001); C. M. Tesch and R. de Vivie-Riedle, Phys. Rev. Lett. **89**, 157901 (2002); D. Babikov, J. Chem. Phys. **121**, 7577 (2004); M. Y. Zhao and D. Babikov, *ibid.* **125**, 024105 (2006); Y. Ohtsuki, Chem. Phys. Lett. **404**, 126 (2005); S. Suzuki, K. Mishima, and K. Yamashita, *ibid.* **410**, 358 (2005); K. Shioya, K. Mishima, and K. Yamashita, Mol. Phys. **105**, 1283 (2007); L. Bomble, D. Lauvergnat, F. Remacle, and M. Desouter-Lecomte, J. Chem. Phys. **128**, 064110 (2008); T. W. Cheng and A. Brown, *ibid.* **124**, 034111 (2006); D. Weidinger and M. Gruebele, Mol. Phys. **105**, 1999 (2007).
[38] J. E. Bayfield, *Quantum Evolution: An Introduction to Time-Dependent Quantum Mechanics* (Wiley, New York, 1999).
[39] K. A. H. van Leeuwen, G. v. Oppen, S. Renwick, J. B. Bowlin, P. M. Koch, R. V. Jensen, O. Rath, D. Richards, and J. G. Leopold, Phys. Rev. Lett. **55**, 2231 (1985).
[40] J. G. Leopold and D. Richards, J. Phys. B **18**, 3369 (1985).
[41] R. Blumel and U. Smilansky, Phys. Rev. Lett. **58**, 2531 (1987).
[42] P. Dietrich and P. B. Corkum, J. Chem. Phys. **97**, 3187 (1992).
[43] B. V. Chirikov, Phys. Rep. **52**, 263 (1979).
[44] R. S. MacKay, J. D. Meiss, and I. C. Percival, Phys. Rev. Lett. **52**, 697 (1984).
[45] D. Bensimon and L. E. Kadanoff, Physica D **13**, 82 (1984).
[46] G. Radons and R. E. Prange, Phys. Rev. Lett. **61**, 1691 (1988).
[47] R. Graham and M. Höhnerbach, Phys. Rev. A **43**, 3966 (1991).
[48] Y. Gu and J. M. Yuan, Phys. Rev. A **36**, 3788 (1987).
[49] S. Krempl, T. Eisenhammer, A. Hübler, G. Mayer-Kress, and P. W. Milonni, Phys. Rev. Lett. **69**, 430 (1992).
[50] H. A. Rabitz and W. Zhu, Acc. Chem. Res. **33**, 572 (2000).
[51] S. Shi and H. Rabitz, Comput. Phys. Commun. **63**, 71 (1991); I. R. Sola, J. Santamaria, and D. J. Tannor, J. Phys. Chem. A **102**, 4301 (1998).
[52] See, for example, P. Gross, H. Singh, H. Rabitz, K. Mease, and G. M. Huang, Phys. Rev. A **47**, 4593 (1993); M. Sugawara and Y. Fujimura, Chem. Phys. **196**, 113 (1995); V. Malinovsky, C. Meier, and D. J. Tannor, Chem. Phys. **221**, 67 (1997); V. S. Malinovsky and D. J. Tannor, Phys. Rev. A **56**, 4929 (1997); Y. Ohtsuki, H. Kono, and Y. Fujimura, J. Chem. Phys. **109**, 9318 (1998); S. Gräfe, C. Meier, and V. Engel, *ibid.* **122**, 184103 (2005); P. Marquetand and V. Engel, J. Phys. B **41**, 074026 (2008).
[53] S. Huang, C. Chandre, and T. Uzer, Phys. Rev. A **74**, 053408 (2006).
[54] G. Ciraolo, C. Chandre, R. Lima, M. Vittot, M. Pettini, C. Figarella, and P. Ghendrih, J. Phys. A **37**, 3589 (2004); C. Chandre, G. Ciraolo, F. Doveil, R. Lima, A. Macor, and M. Vittot, Phys. Rev. Lett. **94**, 074101 (2005).
[55] J. Henkel and M. Holthaus, Phys. Rev. A **45**, 1978 (1992).
[56] For reviews see, E. J. Heller, J. Phys. Chem. **99**, 2625 (1995); O. Brodier, P. Schlagheck, and D. Ullmo, Ann. Phys. (N.Y.) **300**, 88 (2002); S. Keshavamurthy, Int. Rev. Phys. Chem. **26**, 521 (2007).
[57] O. Brodier, P. Schlagheck, and D. Ullmo, Phys. Rev. Lett. **87**, 064101 (2001); C. Eltschka and P. Schlagheck, *ibid.* **94**, 014101 (2005); A. Mouchet, C. Eltschka, and P. Schlagheck, Phys. Rev. E **74**, 026211 (2006).
[58] S. Keshavamurthy, Phys. Rev. E **72**, 045203(R) (2005); S. Keshavamurthy, J. Chem. Phys. **119**, 161 (2003); S. Keshavamurthy, *ibid.* **122**, 114109 (2005).
[59] M. Matsumoto, J. Phys. B **21**, 2863 (1988).
[60] K. M. Christoffel and J. M. Bowman, J. Phys. Chem. **85**, 2159 (1981).
[61] M. D. Feit and J. A. Fleck, J. Chem. Phys. **78**, 301 (1983).
[62] C. Leforestier and R. E. Wyatt, J. Chem. Phys. **78**, 2334 (1983).
[63] K. I. Dimitriou, V. Constantoudis, Th. Mercouris, Y. Komninos, and C. A. Nicolaides, Phys. Rev. A **76**, 033406 (2007).
[64] T. Geisel, G. Radons, and J. Rubner, Phys. Rev. Lett. **57**, 2883 (1986).
[65] N. T. Maitra and E. J. Heller, Phys. Rev. E **61**, 3620 (2000).
[66] C. C. Martens, M. J. Davis, and G. S. Ezra, Chem. Phys. Lett. **142**, 519 (1987); R. B. Shirts and W. P. Reinhardt, J. Chem. Phys. **77**, 5204 (1982); R. Paškauskas, C. Chandre, and T. Uzer, Phys. Rev. Lett. **100**, 083001 (2008); H. Teramoto and T. Komatsuzaki, Phys. Rev. E **78**, 017202 (2008).
[67] S. C. Leasure, F. Milfeld, and R. E. Wyatt, J. Chem. Phys. **74**, 6197 (1981).
[68] R. P. Parson, J. Chem. Phys. **88**, 3655 (1988).
[69] S. Guérin, Phys. Rev. A **56**, 1458 (1997).
[70] O. Bohigas, S. Tomsovic, and D. Ullmo, Phys. Rep. **223**, 43 (1993).